Short title: LecRK-I.1 and insect egg-induced cell death

Corresponding author: Philippe Reymond, Philippe.Reymond@unil.ch

Arabidopsis natural variation in insect egg-induced cell death reveals a role for LECTIN RECEPTOR KINASE-I.1

Raphaël Groux[a], Elia Stahl[a], Caroline Gouhier-Darimont[a], Envel Kerdaffrec[b], Pedro Jimenez-Sandoval [a], Julia Santiago[a], and Philippe Reymond[a,2,3]

[a]Department of Plant Molecular Biology, University of Lausanne, CH-1015 Lausanne, Switzerland

[b]Department of Biology, University of Fribourg, CH-1700 Fribourg, Switzerland

One-sentence summary: A cell-surface receptor controls natural variation of egg-induced cell death in Arabidopsis.

Author contributions: R.G. and P.R. conceived and designed the research. R.G., E.S., and C.G.-D. performed experiments. P.J.S. and J.S. created and analyzed the homology model. R.G., E.K., and P.R. analyzed the data. R.G. and P.R. wrote the manuscript.

[1]This work was supported by the Swiss National Science Foundation (grant no 31003A_169278 to P.R. and grant no. 31003A_173101 to J.S.), EMBO (long term fellowship ALTF 248-2018 to E.K.), and Fondation de Famille Sandoz to J.S and P.J.-S.

[2]Author for contact: Philippe.Reymond@unil.ch

[3]Senior author

The author responsible for distribution of materials integral to the findings presented in this article in accordance with the policy described in the Instructions for Authors (www.plantphysiol.org) is: Philippe Reymond (Philippe.Reymond@unil.ch).

ABSTRACT

In Arabidopsis (*Arabidopsis thaliana*), a hypersensitive-like response (HR-like response) is triggered underneath the eggs of the large white butterfly *Pieris brassicae*, and this response is dependent on salicylic acid (SA) accumulation and signaling. Previous reports indicate that the clade I L-type lectin receptor kinase LecRK-I.8 is involved in early steps of egg recognition. A genome-wide association study (GWAS) was used to better characterize the genetic structure of the HR-like response and discover loci that contribute to this response. We report here the identification of LecRK-I.1, a close homolog of LecRK-I.8, and show that two main haplotypes that explain part of the variation in HR-like response segregate among natural Arabidopsis accessions. Besides, signatures of balancing selection at this locus suggest that it may be ecologically important. Disruption of LecRK-I.1 results in decreased HR-like response and SA signaling, indicating that this protein is important for the observed responses. Furthermore, we provide evidence that LecRK-I.1 functions in the same signaling pathway as LecRK-I.8. Altogether, our results show that the response to eggs of *P. brassicae* is controlled by multiple LecRKs.

Key words: Arabidopsis, genome-wide association study, hypersensitive-like response, insect eggs, LecRK-I.1, *Pieris brassicae*

INTRODUCTION

Although eggs of herbivorous insects deposited on plant leaves are immobile and inert structures, they represent a future threat when hatching larvae start to feed. Plants can detect the presence of eggs and respond by triggering direct and indirect defenses (Reymond, 2013; Hilker and Fatouros, 2015). Direct defenses such as tissue growth and localized cell death lead to reduced egg hatching, egg crushing by surrounding tissues, or egg desiccation and drop off (Shapiro and DeVay, 1987; Doss et al., 2000; Garza et al., 2001; Desurmont and Weston, 2011; Petzold-Maxwell et al., 2011; Fatouros et al., 2014). The production of ovicidal benzyl benzoate at the oviposition site was reported in *Oryza sativa* (Seino et al., 1996; Yamasaki et al., 2003). For indirect defenses, a release of volatiles or changes in leaf surface chemistry attract natural egg predators (Hilker and Meiners, 2006; Fatouros et al., 2012). While these defense mechanisms impact egg mortality individually, some studies found that the co-induction of both direct and indirect defense strategies synergistically impact egg survival (Fatouros et al., 2014). Although such defenses can efficiently reduce insect pressure before damage occurs, one study indicates that these traits may get lost during domestication (Tamiru et al., 2015), like what is observed for other defense-related traits (Chen et al., 2015). Introgression of egg-killing traits in cultivated varieties has been reported in *O. sativa* (Yamasaki et al., 2003; Yang et al., 2014). However, it is still a mostly unexploited strategy due to a lack of mechanistic understanding of these responses at molecular and cellular levels (Reymond, 2013; Fatouros et al., 2016).

Plants from the Brassicales and Solanales orders respond to oviposition through the induction of cell death (Petzold-Maxwell et al., 2011; Fatouros et al., 2014, 2016; Kalske et al., 2014), a process that resembles the hypersensitive response (HR) triggered by certain adapted pathogens. Based on this intriguing similarity, the insect egg-triggered response is considered a hypersensitive-like response (HR-like response) (Reymond, 2013; Fatouros et al., 2014). Recent progress in the study of insect egg-induced necrosis revealed that reactive oxygen species (ROS) and salicylic acid (SA), two major signaling molecules regulating plant immunity, accumulate at oviposition sites (Little et al., 2007; Bruessow et al., 2010; Geuss et al., 2017; Bittner et al., 2017; Bonnet et al., 2017). In Arabidopsis (*Arabidopsis thaliana*), cell death induction upon crude egg extract (EE) treatment was reduced in mutants impaired in SA biosynthesis and signaling (Gouhier-Darimont et al., 2013). In *Brassica nigra*, only plants expressing HR-like symptoms displayed elevated *PR1* transcript levels, a widely used SA marker gene, again suggesting that induction of the HR-like response requires SA accumulation (Fatouros et al., 2014). These results indicate that the response to insect eggs is

similar to pathogen-triggered immunity (PTI), as demonstrated in Arabidopsis (Gouhier-Darimont et al., 2013). However, knowledge of elicitor-receptor pairs involved in plant response to eggs is lacking. We recently identified egg-derived phosphatidylcholines as elicitors of Arabidopsis immune responses and showed that the L-type LecRK-I.8 is an early signaling component of *Pieris brassicae* egg-induced responses, thereby constituting a potential candidate for the perception of these elicitors (Gouhier-Darimont et al., 2019; Stahl et al., 2020). Lectin-like receptor kinases (LecRKs) have been implicated in a myriad of immune-related processes such as PTI (Takahashi et al., 2007), chitin perception (Miya et al., 2007), e-(extracellular) ATP and $eNAD^+$/$eNADP^+$ perception (Choi et al., 2014; Wang et al., 2017; Wang et al., 2019; Pham et al., 2020), bacterial short chain 3OH-FA perception (Kutschera et al., 2019), and insect resistance (Gilardoni et al., 2011; Liu et al., 2015). Interestingly, a recent study exploiting natural variation in parasitoid attraction following oviposition in maize identified a locus containing a leucine-rich repeat receptor kinase (Tamiru et al., 2020).

Although insect eggs trigger a PTI-like response in Arabidopsis, identification of early and late components is still needed. Transcriptome changes after *P. brassicae* oviposition and pathogen infection are similar but not identical, suggesting some level of specificity (Little et al., 2007). In support of this hypothesis, ROS production following *P. brassicae* EE treatment was independent on the NADPH oxidases RBOHD/F (Gouhier-Darimont et al., 2013), while this pathway is crucial for pathogen-triggered ROS accumulation (Torres et al., 2002; Morales et al., 2016). Moreover, a *lecrk-I.8* mutant plant did not show altered resistance to a bacterial pathogen (Gouhier-Darimont et al., 2019), suggesting that LecRK-I.8 may be specifically involved in egg signaling responses. To gain more molecular insight into the insect egg-induced response, we used the existing natural variation in EE-triggered HR-like response in Arabidopsis and performed a genome-wide association study (GWAS) using a set of 295 natural accessions. We found a peak of association on chromosome 3 encompassing the clade I *LecRK-I.*1, a homolog of *LecRK-I.8*. Subsequent experimental validation showed that LecRK-I.1 is specifically involved in the regulation of cell death following insect egg perception, hence providing an additional component of this immune response.

RESULTS

Arabidopsis accessions display natural variation in response to *P. brassicae* eggs

We observed that Arabidopsis accessions display varying degrees of HR-like response after 5 days of treatment with *P. brassicae* EE (Fig. 1A), corresponding to the hatching time of real eggs. The existence of natural variation for this defense-related trait suggests that it is under genetic control, consistent with previous reports (Gouhier-Darimont et al., 2013, 2019). While most leaves exhibited some degree of chlorosis, symptoms usually ranged from no visible symptom to the formation of large patches of cell death (Fig. 1B). Moreover, symptoms were most of the time restricted to the area of EE application, but could exceptionally grow larger for necrosis. This scoring scheme allows an easy quantification of the HR-like response (Fig. 1C). To verify that application of *P. brassicae* EE mimics the reaction induced by real eggs, we tested whether naturally oviposited eggs could also induce some degree of variation in HR-like responses. In several accessions, we observed the formation of chlorotic or necrotic tissue localized around and underneath the egg clutches after 5 days (Fig. 1D). This was generally associated, although not completely, with the severity of symptoms observed after EE treatment (Supplemental Fig. S1). Contrasting symptom responses between oviposition and EE treatment could be due to the presence of the protective shell that may delay the release of endogenous elicitors (Bruessow et al., 2010; Stahl et al., 2020). However, since defense-inducing activity has also been attributed to compounds associated with the secretion attached to the eggs (Paniagua et al., 2020), other reasons, including different strengths of egg attachment to the cuticle, may also explain such variability. Because conducting such a large screen with butterflies was practically challenging, we thus set conditions for a GWAS using EE treatment and performed initial tests on three selected accessions, using Col-0 as a control. Based on these experiments, we used short-day grown plants (10L:14D), treated three leaves per plant with EE diluted 1:1 with water, and scored symptoms after five days (Supplemental Fig. S2A-C). Because such experiment requires a large amount of EE, this allowed us to maximize the number of plants treated per accession and per block, although the use of undiluted EE and/or long day conditions tend to increase symptom strength (Supplemental Fig. S2A-C).

Identification of a genetic locus associated with *P. brassicae* egg-induced symptoms

Broad sense heritability (H^2), which estimates the phenotypic variance that is genetically encoded, was high for symptom score ($H^2 = 0.56$). This finding is consistent with previously reported H^2 values for defense phenotypes (Yang et al., 2017). GWA mapping using

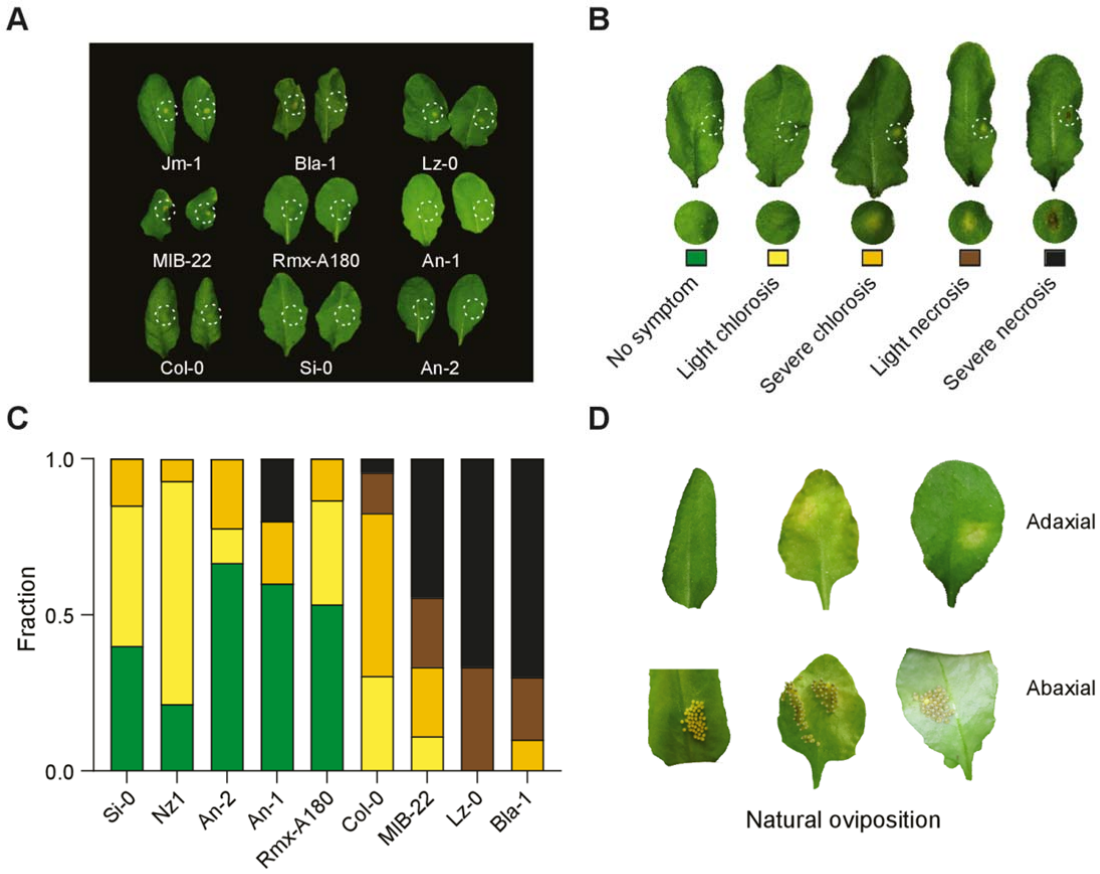

symptom score for 295 accessions and a fully imputed genotype matrix (Togninalli et al., 2018) revealed the existence of two loci associated with the degree of cell death induced by EE (Fig. 2A). One peak of association was found on chromosome 2 ($-\log_{10} P = 15.96$) and constitutes the basis for another study (R. Groux and P. Reymond, unpublished data). Besides this peak, we observed the existence of another significantly associated marker ($-\log_{10} P = 7.59$, position 16633422) on chromosome 3 (Fig. 2A), which explains 9.56% of the phenotypic variance. This peak is also present when temporal effects are considered by normalizing symptom scores to a weekly set of Col-0 control plants (Supplemental Fig. S3B,C and Methods). By taking a closer look at this genomic region, we found that this marker is in the coding sequence of the *L-TYPE LECTIN RECEPTOR KINASE-I.1* (At3g45330) (Fig. 2B). Interestingly, this genomic locus encompasses five other closely related clade I *LecRK* genes, *LecRK-I.2* to *LecRK-I.6*. We found that high linkage disequilibrium (LD) with other surrounding markers was only observed for SNPs found in the gene sequence of *LecRK-I.1* (Fig. 2B), suggesting that this gene may be causal for the differences in HR-like responses elicited by EE. We then determined whether this locus was previously identified in other publicly available GWAS. According to the araGWAS database

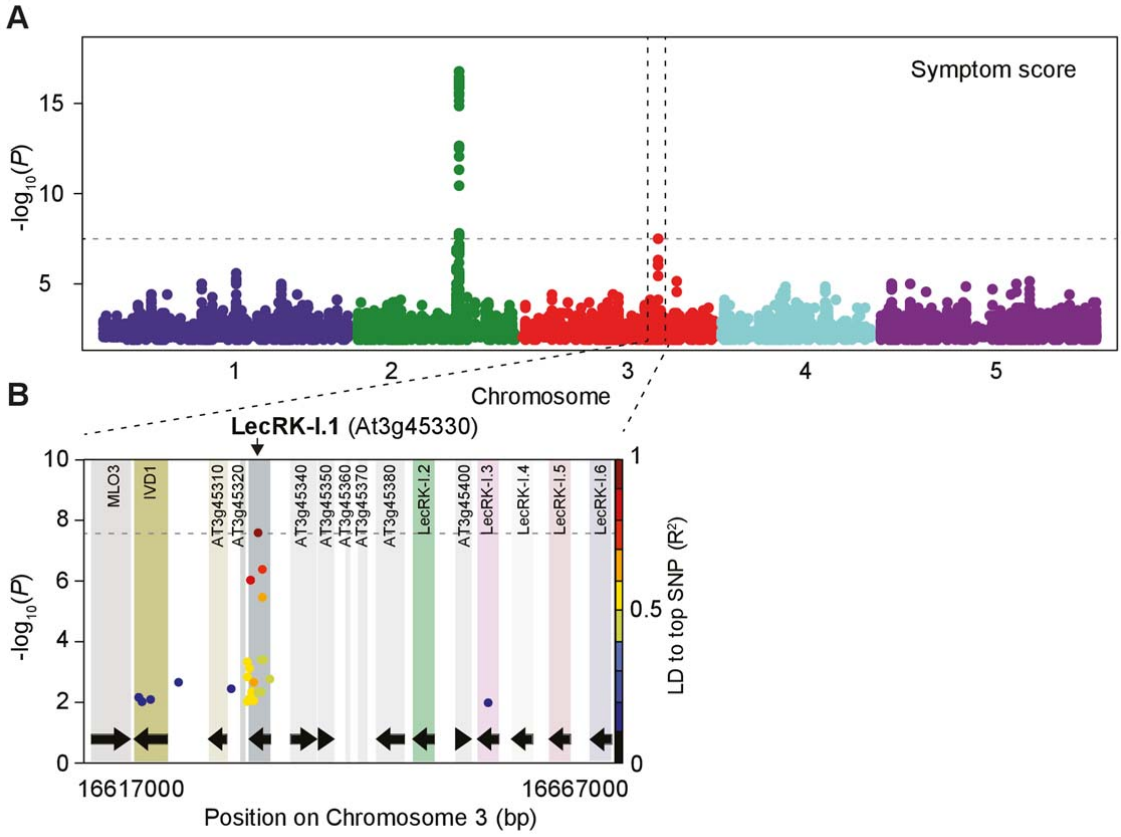

(Togninalli et al., 2018), markers at the *LecRK-I.1* locus are not associated with any of the defense-related or developmental phenotypes available, suggesting that it may play a specific role during the *P. brassicae* egg-induced response (Supplemental Fig. S4).

LecRK-I.1 is involved in EE-induced cell death

To test whether clade I LecRKs found in this region could be involved in the response to *P. brassicae* EE, we used T-DNA insertion lines for single LecRKs and measured alterations in different egg-induced responses. Additionally, to explore whether redundancy among these genes exists, we used CRISPR-Cas9 technology to delete the entire cluster of *LecRK-I.1* to *LecRK-I.6* (hereafter named *ccI.1-I.6*). The symptom score was significantly lower than Col-0 in *lecrk-I.1* mutant but not in knockout lines from homologs (Fig. 3A). Consistently, deletion of the gene cluster led to symptom reduction like that observed in *lecrk-I*. We then quantified cell death at the site of EE application by trypan blue staining and observed a similar pattern (Fig. 3B). These results show that *LecRK-I.1*, but not other homologs from the genomic cluster, is involved in induction of the HR-like responses elicited by EE.

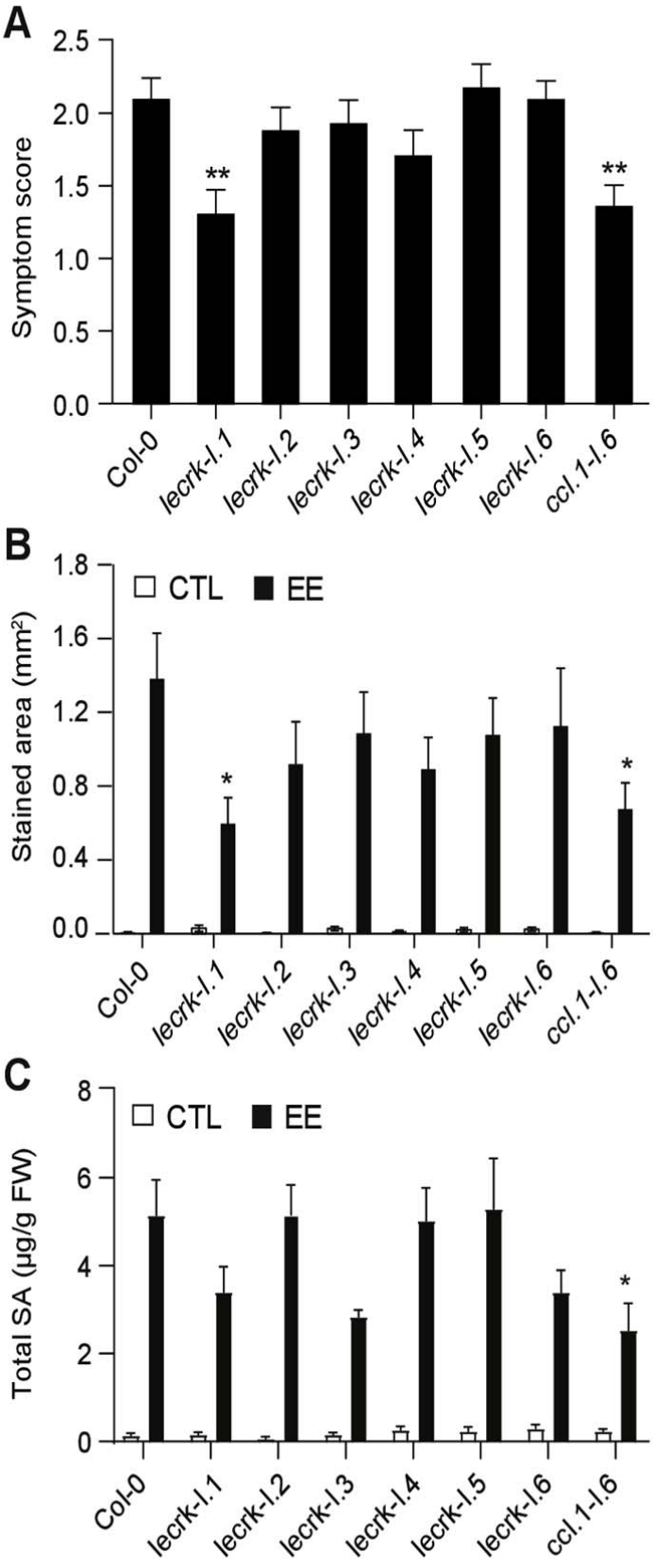

Because altered SA signaling in the *lecrk-I.1* mutant could account for the reduction in

cell death, we next quantified SA levels in plant treated with EE for 3 days. Total SA levels were reduced in *lecrk-I.1* after 3 days of treatment compared to wild-type plants (Fig. 3C). Interestingly, we observed a similar result in *lecrk-I.6* and *lecrk-I.3* mutants, indicating that multiple LecRKs may regulate SA accumulation. Removal of all six *LecRKs* in the *ccI.1-I.6* line resulted in significantly lower SA levels after EE treatment (Fig. 3C), further supporting that one or more clade I LecRKs may participate in EE-induced SA accumulation.

Finally, to further validate the role of LecRK-I.1, we exposed *lecrk-I.1* and *ccI.1-I.6* lines to oviposition by *P. brassicae*. Symptom scores 4.5 days after egg laying were lower for both mutant lines (Fig. 4A). This reduction was however not significant, suggesting that the contribution of LecRK-I.1 to the egg-elicited HR-like response is weaker than to the EE-elicited HR-like response, for reasons that need further investigation. However, SA accumulation and cell death intensity were significantly reduced in the mutants (Fig. 4B, C), confirming the data obtained with EE. Altogether, these results thus demonstrate a role for LecRK-I.1 in the regulation of SA accumulation and cell death after EE treatment and natural oviposition.

LecRK-I.1 haplotypes correlate with egg-induced symptoms

The finding that natural variation in *LecRK-I.1* is associated with the strength of HR-like responses elicited by EE among Arabidopsis accessions indicates that variants of this gene may alter protein function(s) or gene expression. As mentioned, we observed that a single marker reached genome-wide significance (SNP3; Chr. 3, 16633422) while four other SNPs had intermediate *P*-values ($-\log_{10} P > 4$), all within the coding sequence of *LecRK-I.1* (Fig. 5A, B). Interestingly, three out of five SNPs result in amino acid changes: one (SNP5) in the putative carbohydrate-binding lectin-like domain (I228R), and two in the kinase domain (R356K, SNP3; I602V, SNP1), while the two other associated markers lead to silent mutations (Fig. 5B). Additionally, linkage analysis revealed that all markers are in moderate to strong LD with SNP3 (Fig. 5A). Since we do not know which marker might be causal, we considered haplotypes defined by SNP1-5. We next determined that at least 5 haplotypes are present in the population used for GWAS mapping (Fig. 5C), with two of them being present at rather high frequency compared to the other three (H2, 30.51%; H5, 58.64%; H1, H3, and H4 <7%). We observed that the distribution of symptom score was similar between haplotypes having variants in the lectin domain, suggesting that these variants might not impact this response. However, non Col-0 alleles for markers in the kinase and lectin domains together are associated with significantly lower symptoms (H2 vs H5, Fig. 5C). Together with

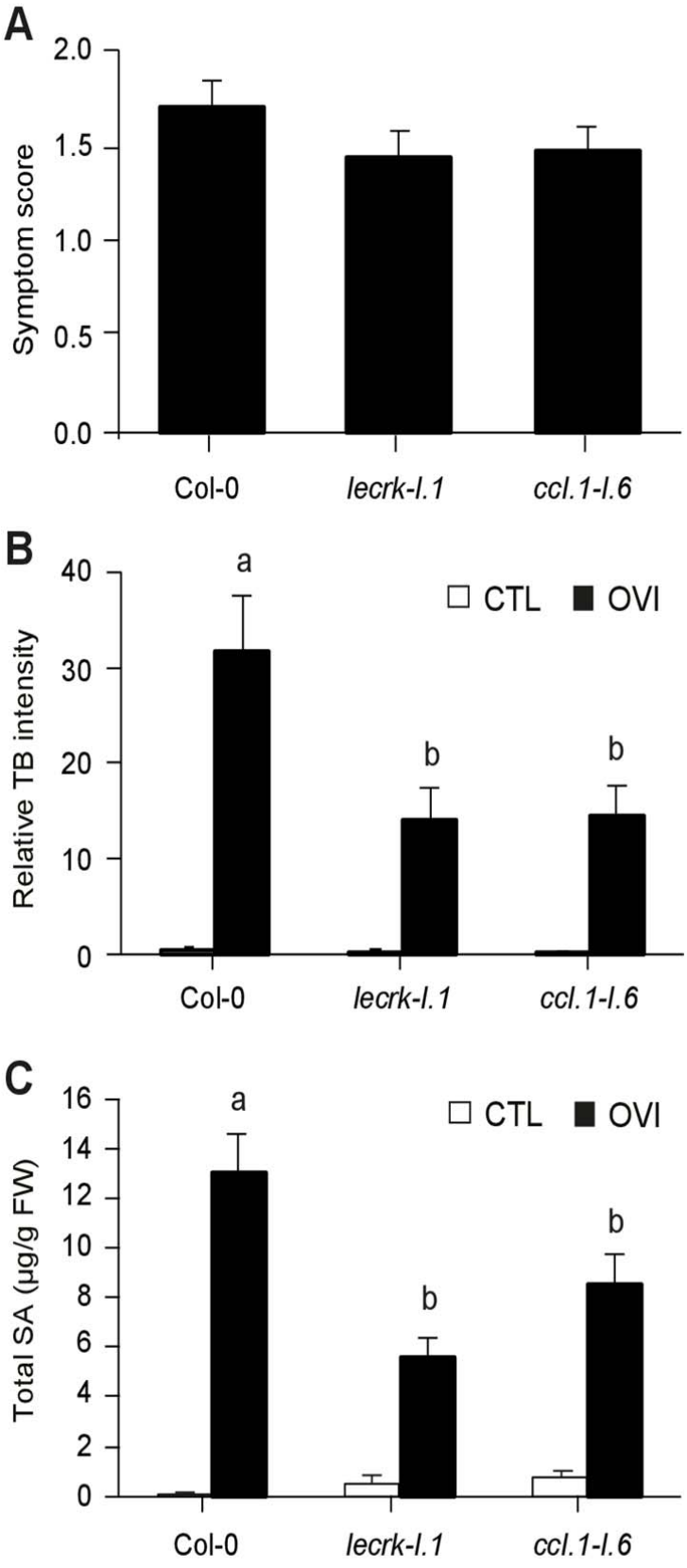

the previous finding, these results potentially indicate that differential kinase function may

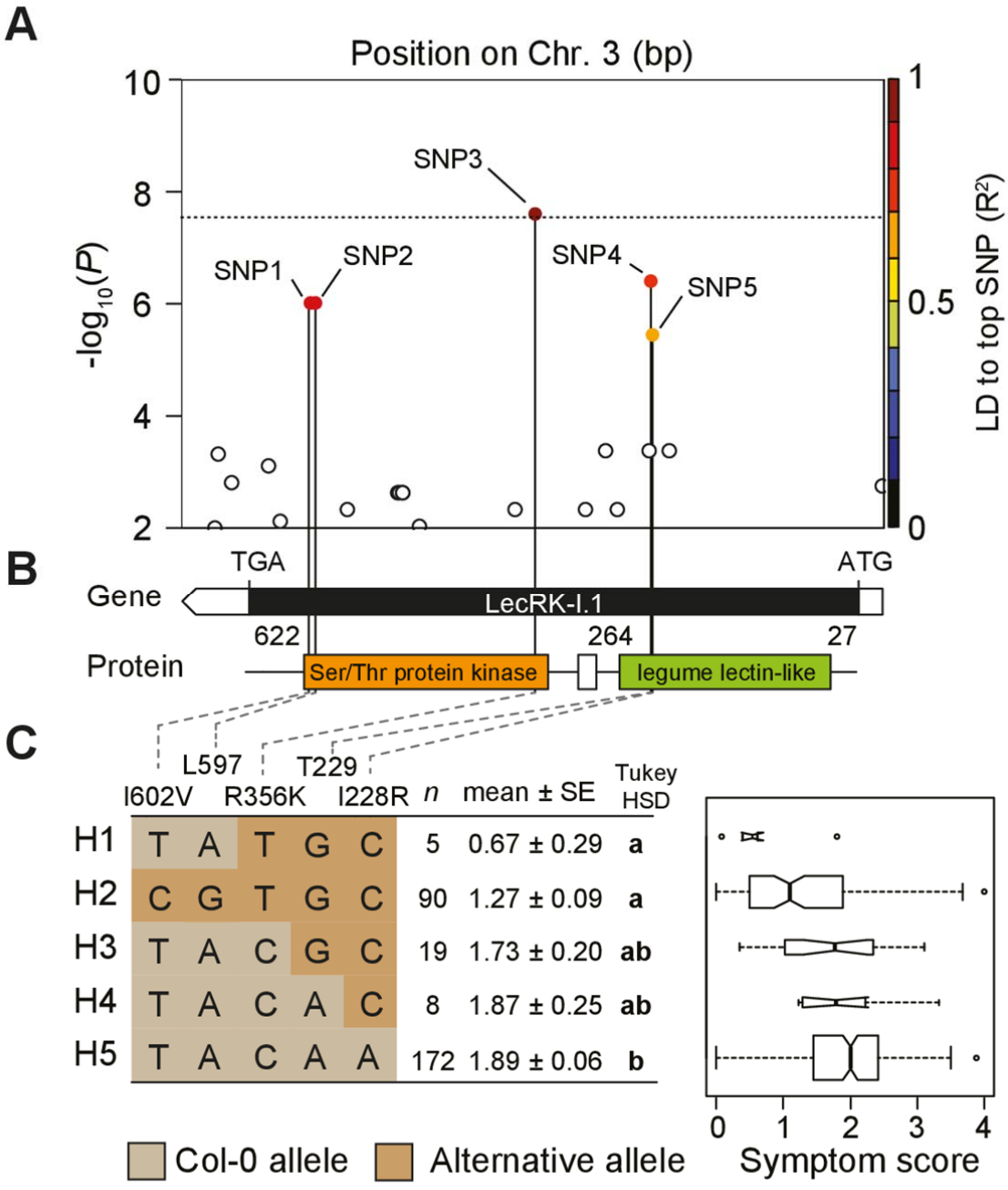

underlie natural variation in EE-induced cell death. To explore this possibility, we examined whether these variants are found in functional subdomains of the kinase. Based on annotation from the UNIPROT database, we found that R356K lies close to the predicted ATP binding site. We then performed homology-based modeling using SWISSMODEL (https://swissmodel.expasy.org) to predict the 3D topology of the LecRK-I.1 kinase domain and to assess whether this amino acid change could potentially alter kinase function. In

protein kinases, the active site lies in the cleft between two lobes, termed as N-lobe and C-lobe. One important element for catalysis is the glycine-rich loop that contains the GxGxxG motif, the most flexible region of the N-lobe. In its closed conformation, this motif folds over the γ-phosphate of ATP and orients it for catalysis (Taylor and Kornev, 2011). The residue R356 corresponds to the first x on the GxGxxG motif (GRGGFG in LecRK-I.1). As shown in the model in Supplemental Fig. S5, the side chain of this residue is oriented to the solvent and only the backbone is helping in positioning the ATP at the catalytic cleft. The orientation of the side chain and the "ATP-backbone coordination" by the second residue in the GxGxxG motif (R356 in LecRK-I.1) are conserved in all the available kinase structures that share this motif (PDB ID codes: 5LPV, 6CTH, 3HGK, 5XD6, 6BFN, 6EG9, 3TL8). Thus, it is unlikely that the R356K variant could affect the canonical kinase function of LecRK-I.1. However, it was recently reported that the kinase domain of the co-receptor SERK3/BAK1 undergoes proteolytic processing between residues R and G at the GxGxxG motif (GRGGFG in BAK1, the same sequence as in LecRK-I.1) by the bacterial effector HopB1 to inhibit plant defenses, and that the substitution of R to K in the GxGxxG motif prevents cleavage of BAK1 by HopB1 (Li et al., 2016). Zhou et al. (2019) proposed that homeostasis through proteolytic processing of SERKs kinase domain by yet unknown host proteases is a key mechanism to control plant growth and immunity. Thus, whether LecRK-I.1 is subject to egg-induced proteolysis is an intriguing hypothesis that deserves future investigation.

The other kinase variant (I602V) and the lectin domain variant (I228R) appeared to be outside the ATP binding site in the kinase domain, and outside the sugar-binding site of the lectin domain, and are also solvent exposed (Supplemental Fig. S5). These results suggest that the identified variants may not be involved in canonical kinase or receptor function based on knowledge obtained from homologous proteins. We also determined whether multiple independent frame shifts and/or premature stop codon may be present in natural variants at this locus, potentially leading to the production of a truncated protein. We found that 18% of the sequenced accessions (23/125) possessed such variants (Supplemental Fig. S6A), yet this does not correlate with any difference in symptom distribution independently of the haplotype considered (Supplemental Fig. S6B). Moreover, premature STOP codons occurred within the first 20 amino acids of the sequence. This suggests that these frame shifts and premature stops may not necessarily lead to the production of non-functional proteins, possibly through the existence of alternative start sites. Collectively, our results point to a role for variation in the *LecRK-I.1* gene sequence in modulating HR-like responses elicited by EE. However, the link between variation in the coding of this gene and the resulting phenotype is still unclear.

LecRK-I.1 expression is haplotype specific but does not correlate with symptom severity

The absence of any obvious impact of the variation identified within the *LecRK-I.1* coding sequence may indicate that an alternative process is involved. We determined whether differences in gene expression may correlate with haplotype identity and HR-like symptoms by measuring *LecRK-I.1* transcript levels following EE treatment in 40 accessions with high or low symptoms. Gene expression was highly variable in the accessions surveyed, and expression was barely detectable in certain lines (Supplemental Fig. S7). We found that the two most frequent haplotypes were not associated with differential *LecRK-I.1* expression after EE treatment, although one of the minor haplotypes displayed comparatively lower transcript levels (Fig. 6A). Despite this haplotype-specific expression pattern, we found no correlation between symptom score and *LecRK-I.1* expression levels in the surveyed accessions (Fig. 6A, B). Analysis of publicly available RNA-seq data from different accessions (see methods) allowed for a similar analysis using SNP3 to split the data. Consistent with our experiments, none of the alleles at this position was associated with altered *LecRK-I.1* transcript levels (Supplemental Fig. S8). Altogether these results suggest that variation in *LecRK-I.1* expression does not account for the variation in HR-like responses elicited by EE between accessions.

Signatures of selection at the LecRK-I.1 locus

Based on the haplotype analysis, we found that only five *LecRK-I.1* haplotypes segregate in the mapping population used in this study. To get a closer look, we calculated haplotype frequencies using SNP1-5 described earlier. As mentioned before, two haplotypes appear to be present at high frequencies (H2, 30.51%; H5, 58.64%), while the three remaining haplotypes are much less frequent (< 7%, Fig. 7A). This could indicate that haplotypes are distributed in two subpopulations due to adaptation to a type of environment or that selection is acting at this locus and is maintaining variation. To disentangle these hypotheses, we constructed a cladogram representing genetic distance by using the kinship matrix used during the GWA mapping and superimposed haplotype identity for each accession (Fig. 7B). While it does appear that some low frequency haplotypes could be specific to certain geographical locations, the two major haplotypes appear to have a very broad distribution in the entire Arabidopsis population used for mapping (Supplemental Fig. S9). The absence of any obvious link with phylogenetical or geographical history suggests that selection may be acting at this locus. To test the hypothesis that the *LecRK-I.1* gene sequence does not evolve

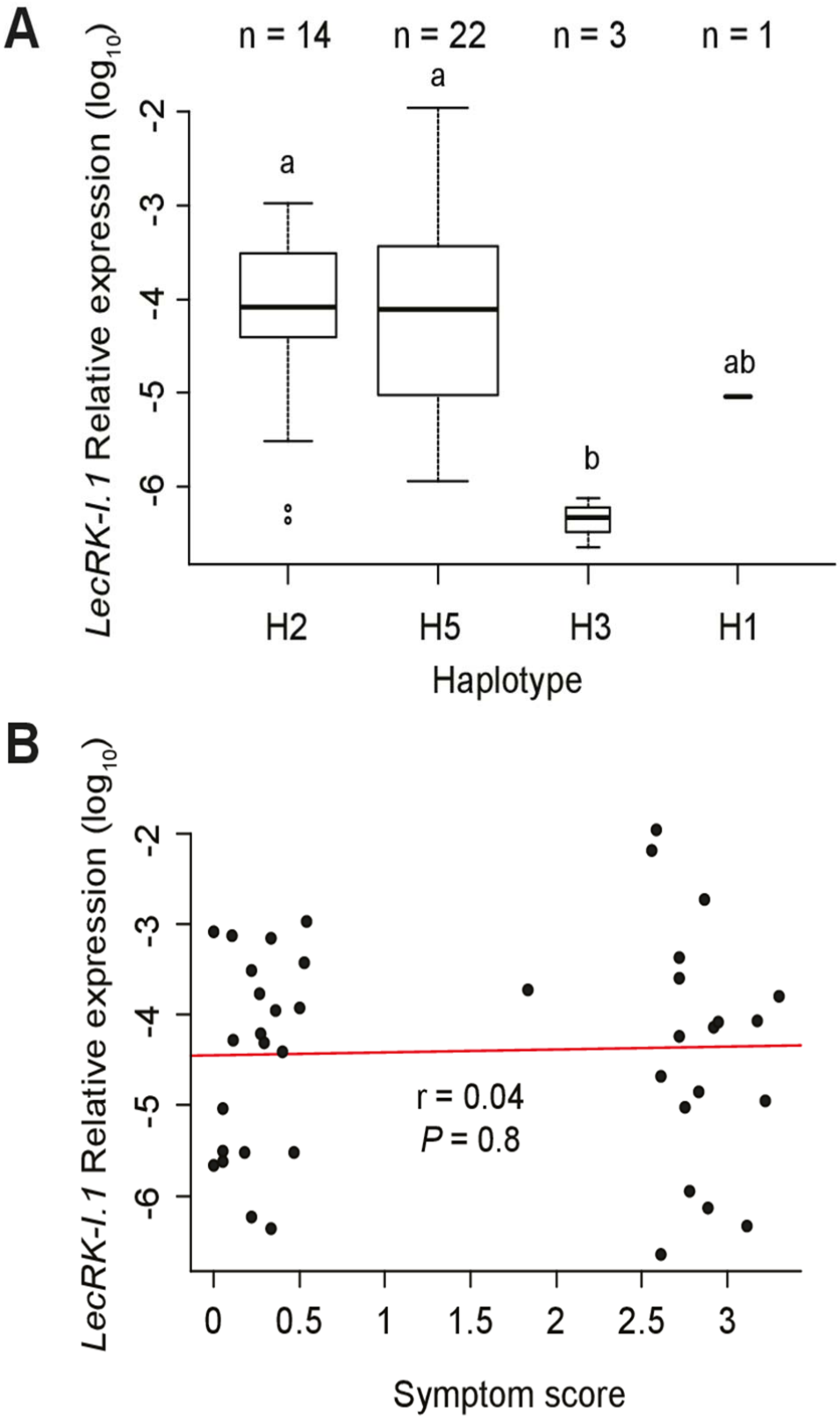

neutrally, we measured Tajima's D statistic along the coding sequence by using a sliding

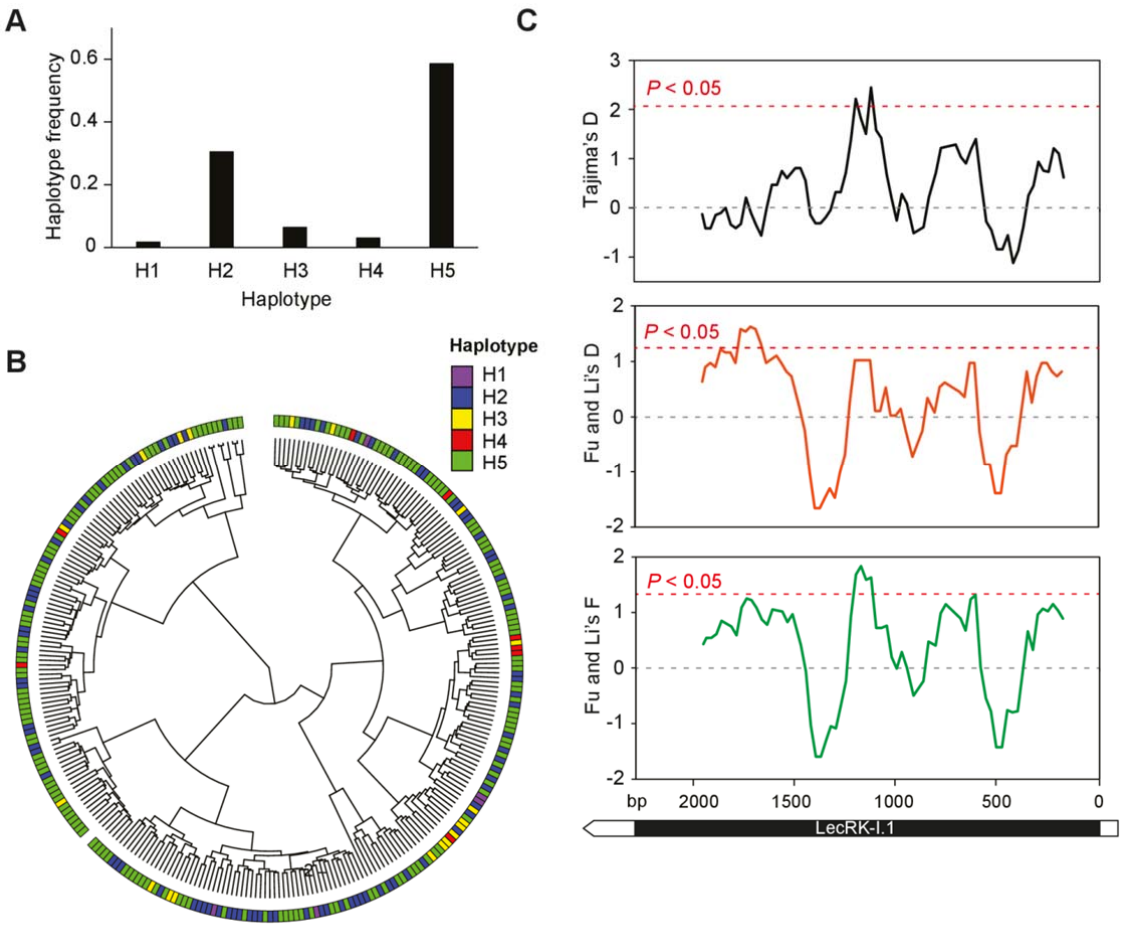

window (Fig. 7C). Tajima's D compares the observed frequency of variants to those expected for a similar sequence evolving neutrally (Tajima, 1989), thereby indicating any departure from neutrality. We found that Tajima's D was mainly positive along the gene sequence of *LecRK-I.1*, and two short stretches were significantly positive (Fig. 7C). This result is indicative that *LecRK-I.1* might not evolve neutrally. Also, we found that nearly all genes surrounding *LecRK-I.1* displayed negative Tajima's D values when computed over a 50 kb region (Supplemental Fig. S10). Because Tajima's D is sensitive to demographic history, we also performed a sliding window analysis of Fu and Li's D and F statistics, which considers the species history by including an outgroup (*Arabidopsis lyrata*). We observed that the pattern and sign of Fu and Li's statistics were very similar to Tajima's D (Fig. 7C), further supporting the hypothesis that this locus is not evolving neutrally.

LecRK-I.1 and LecRK-I.8 function in the same pathway

Based on the previously reported identification of LecRK-I.8, a close homolog of LecRK-I.1 (Bouwmeester and Govers, 2009; Hofberger et al., 2015), as an early component of egg-

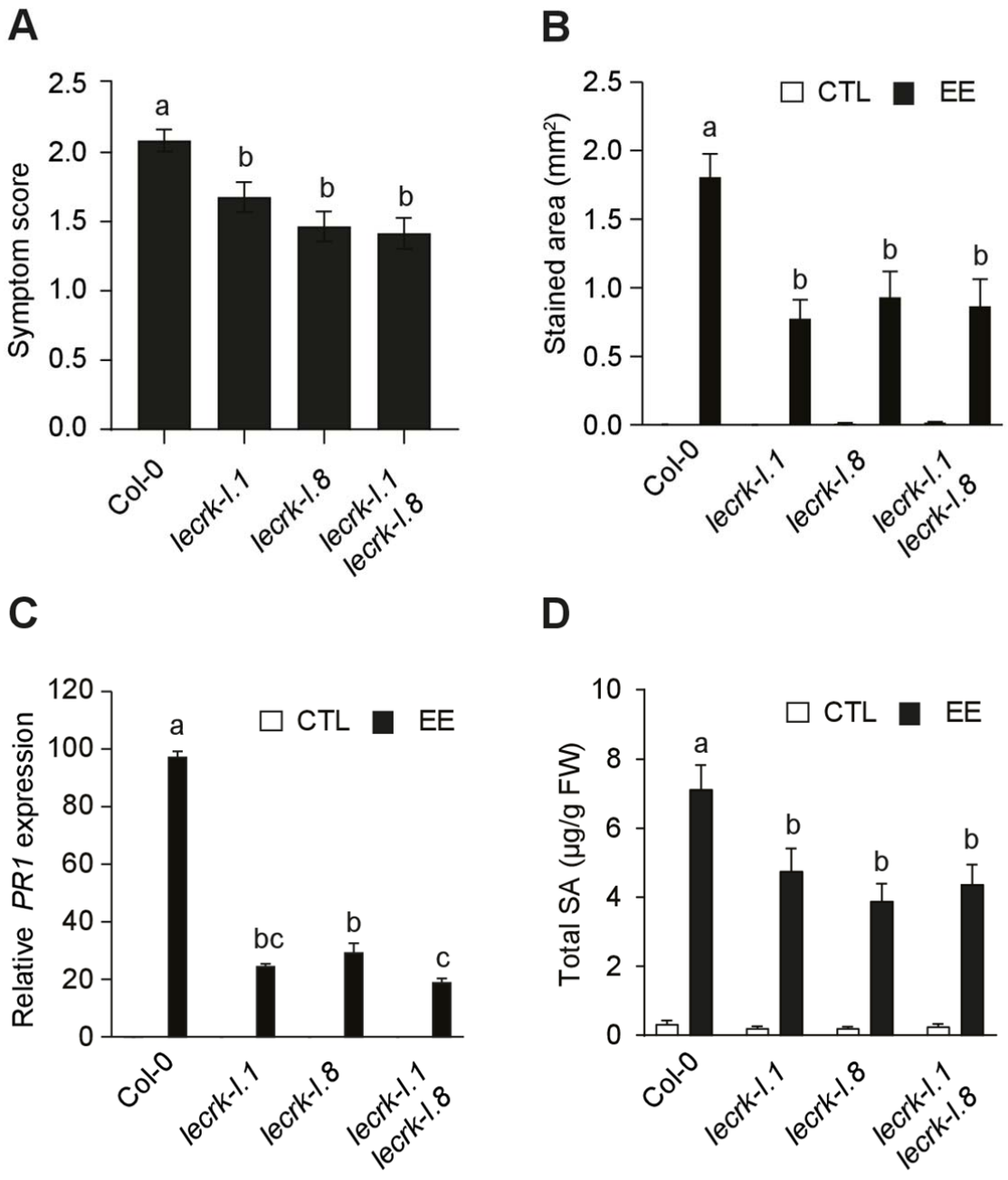

triggered signaling (Gouhier-Darimont et al., 2019), we wondered whether both genes may function in the same signaling cascade or if they are involved in parallel pathways. We crossed *lecrk-I.1* with *lecrk-I.8* and measured EE-induced responses in the single and double mutants. Both single mutants displayed a similar reduction of HR-like symptoms, *PR1* expression, and SA accumulation after EE treatment. However, the double mutant did not show further reduction of these responses, strongly suggesting that LecRK-I.1 and LecRK-I.8 act in the same pathway (Fig. 8A-D).

DISCUSSION

The recent description of LecRK-I.8 as an upstream regulator of insect egg-triggered signaling opened the exciting possibility that it could be involved in egg perception (Gouhier-Darimont et al., 2019). However, several phenotypes including cell death were not abolished in the *lecrk-I.8* mutant, indicating a potential redundancy with other homologs or that LecRK-I.8 works as a modulator of the response. Indeed, expression of all other clade I *LecRKs* is also induced following EE treatment (Gouhier-Darimont et al., 2019). We describe here the identification of LecRK-I.1 as a component of the EE-triggered signaling pathway in Arabidopsis that affects the induction of HR-like responses during this interaction. Although we had previously observed that EE-induced *PR1* expression was lower in the *lecrk-I.1* mutant, the data did not reach statistical significance (Gouhier-Darimont et al., 2019). Having identified LecRK-I.1 in the GWAS, we further analyzed this mutant in the same experimental conditions and confirmed reduced expression of *PR1* in three new independent biological replicates. Since the contribution of LecRK-I.1 to EE-induced *PR1* expression is only partial, we postulate that compensation by other members of the LecRK clade I can happen in some experiments and mask the effect of single members. We also show that a knockout mutant of *LecRK-I.1* leads to reduced HR-like symptoms and cell death following *P. brassicae* oviposition and EE treatment, while SA accumulation is reduced. Moreover, double knock-out of both *LecRK-I.1* and *LecRK-I.8* did not result in a further reduction of EE-elicited HR-like symptoms, *PR1* expression, and SA accumulation, suggesting that both genes function in the same transduction pathway or are part of the same complex. Other clade I *LecRK* mutants showed reduced SA levels and this was further confirmed by deleting all six genes clustered in the same locus. These results suggest that several clade I LecRKs are involved in the response to eggs and control different aspects of this pathway. It is noteworthy that only LecRK-I.1 and LecRK-I.8 affect the induction of cell death following egg perception, whereas only the *LecRK-I.1* locus displays natural variation. Further work will be needed to evaluate the contribution of each homolog to the plant response to oviposition. Besides, whether LecRK-I.1 and homologs also play a role in the typical pathogen-induced HR needs further investigation.

Despite the absence of known ligands for LecRK-I.1 and most other clade I LecRKs, it has been reported that LecRK-I.1 possesses a putative RGD-binding motif and that it may participate in plasma membrane-cell wall interactions (Gouget et al., 2006). Whether insect eggs trigger changes in cell wall properties is not known, but epicuticular wax patterns were altered upon *P. brassicae* oviposition on Arabidopsis (Blenn et al., 2012). In contrast to

lectins, LecRKs show poorly conserved sugar-binding residues and it is therefore unlikely that they bind carbohydrates (Bouwmeester and Govers, 2009). However, the conserved hydrophobicity of the resulting cavity could recognize more hydrophobic ligands. Given the lipidic nature of egg-derived inducing compounds (Bruessow et al., 2010; Gouhier-Darimont et al., 2019; Stahl et al., 2020), this would be consistent with a role for L-type LecRKs in egg perception. Recently, the G-type LecRK LORE was found to bind to medium chain 3-OH fatty acids that trigger LORE-dependent immunity (Kutschera et al., 2019), further supporting the hypothesis that some LecRKs may recognize hydrophobic ligands from insect eggs. Alternatively, LecRKs could also be involved in the perception of secondary signals such as DAMPs as suggested by the identification of LecRK-I.8 and LecRK-VI.2 as potential receptors for $eNAD^+$ and $eNADP^+$ (Wang et al., 2017; Wang et al., 2019), and LecRK-I.9 and LecRK-I.5 as eATP receptors (Choi et al., 2014; Pham et al., 2020). Here, we provide evidence that LecRK-I.1 and LecRK-I.8 function as components of the same pathway/complex. This suggests that LecRK-I.1 might serve as a secondary signaling hub that controls LecRK-I.8-dependent cell death. Whether LecRK-I.1 binds egg-derived elicitors alone or with LecRK-I.8 is an intriguing hypothesis that deserves further research. A more detailed evaluation of egg-triggered phenotypes in single and double mutants will help address this hypothesis.

We found that natural variation in the *LecRK-I.1* gene sequence was associated with HR-like responses elicited by EE, consistent with the phenotype observed in the *lecrk-I.1* mutant. Two main haplotypes of this gene segregate at the population level and one variant (SNP3) in the kinase domain was significantly associated with HR-like symptoms. Evaluation of *LecRK-I.1* expression in accessions indicates that transcript levels are not associated with symptom severity, therefore suggesting that functional variation in the LecRK-I.1 protein sequence modulates the HR-like responses elicited by EE. Unfortunately, our analysis suggests that none of the identified variants would substantially affect the lectin binding pocket or the kinase domain. *In vitro* kinase assay using different variants of the kinase domain may help address this question directly. Recently, LecRK-VI.2 was shown to interact with the immune co-receptor BAK1 (Huang et al., 2014; Wang et al., 2019) and both proteins are necessary for $eNAD^+$/$eNADP^+$-induced signaling. Given the critical nature of such interactions for signal transduction, solvent-exposed natural variants associated with reduced HR-like symptoms could affect the binding of putative co-receptors and partners of LecRK-I.1. Moreover, LecRK homo- and heterodimerization was reported (Bellande et al., 2017;

Wang and Bouwmeester, 2017), suggesting that a similar process might underlie LecRK-I.1 function and such interaction may be affected in the natural variants identified.

At the genomic level, L-type *LecRKs* are organized in clusters of tandem repeats that arose through local and whole genome duplication events (Hofberger et al., 2015). Clade I *LecRK* genes appear to be mostly Brassicaceae-specific (Hofberger et al., 2015; Wang and Bouwmeester, 2017) and most of them are involved in immunity. *LecRKs* originated following the At-α whole genome duplication event (50 Mya), and LecRKs that were duplicated during this period show signs of positive selection (Hofberger et al., 2015). Consistent with this study, we found that the two major *LecRK-I.1* haplotypes segregate at intermediate to high frequencies, independently of any obvious geographical or phylogenetical pattern. The co-occurrence of such diverged polymorphisms indicates that they could be ancient and may have been maintained by selection. Consistent with the latter hypothesis, we found that the *LecRK-I.1* locus does not seem to evolve neutrally, as indicated by positive Tajima's D, and Fu and Li's D/F statistics. Positive values for these statistics are considered as signatures of balancing selection, a selection that is observed in immunity-related or resistance genes for instance (Bakker et al., 2006; Vila-Aiub et al., 2011; Huard-Chauveau et al., 2013; van Velzen and Etienne, 2015; Ariga et al., 2017). Balancing selection collectively refers to processes by which genetic variation is maintained in a population, as opposed to purifying and positive selection that reduces variation (Delph and Kelly, 2014; Wu et al., 2017). Different selective processes can ultimately lead to the maintenance of genetic variation such as overdominance (or heterozygote advantage), frequency-dependent selection, or environmental heterogeneity (spatially varying selection). Identification of the mode of balancing selection acting at this locus deserves further investigation. Nevertheless, the fact that *LecRK-I.1* displays signatures of balancing selection highlights the potential ecological importance of this gene in natural Arabidopsis populations.

P. brassicae and Arabidopsis provide a good model system to investigate the mechanistic aspects of egg perception and plant responses. However, Arabidopsis may not be the preferred host of *P. brassicae* in nature. Although *P. brassicae* readily oviposits on Arabidopsis plants in the lab, it prefers other brassiceous species when given the choice (Griese et al., 2020). The ecological and evolutionary relevance of natural variation in HR-like responses elicited by EE in Arabidopsis will thus need further research to identify insect species that drive this phenomenon. Besides, although we recently showed that elicitors are freely released from *P. brassicae* eggs (Stahl et al., 2020), the use of crushed egg extract may expose the plant to additional components that normally do not reach the plant surface.

LecRK-I.5/I.9 and LecRK-I.8 and have been shown to bind ATP or NAD, respectively, implying that these clade I members may detect DAMPs (Choi et al., 2014; Wang et al., 2017; Wang et al., 2019; Pham et al., 2020). LecRK-I.1 could not compensate for the lack of LecRK-I.5 in ATP responses and thus is unlikely to respond to this DAMP (Pham et al., 2020). However, the possibility that our study unveiled a role for LecRK-I.1 in DAMP perception cannot formally be ignored and will deserve additional studies. Finally, while the results presented here shed more light on the understanding of the induction of the cell death response in Arabidopsis, it is not known whether LecRK-I.1 also plays a role in crop species such as cabbage or canola. Interestingly, induction of an HR-like response in *B. nigra* also correlates with higher egg parasitism, indicating that both defense mechanisms may be under a similar regulation (Fatouros et al., 2014). More study of this region in other Brassicaceae and a screen of available germplasms for natural variation may demonstrate a role for clade I LecRKs in sister species.

MATERIALS AND METHODS

Plant materials and growth conditions

All experiments described here were carried out in Arabidopsis (*Arabidopsis thaliana*). Plants were grown in growth chambers in short day conditions (10 h light, 22°C, 65% relative humidity, 100 µmol m^{-2} s^{-1}) and were 4 to 5 weeks old at the time of treatment. The colony of Large White butterfly *Pieris brassicae* was reared on *Brassica oleracea* in a greenhouse (Reymond et al., 2000).

Accessions used for GWAS mapping were obtained from the NASC stock center and are listed in Supplemental Table S1. T-DNA insertion lines for *lecrk-I.1* (SALK_052123), *lecrk-I.2* (SAIL_847_F07), *lecrk-I.3* (SALK_087804C), *lecrk-I.4* (SALK_091901), *lecrk-I.5* (GABI_777H06), *lecrk-I.6* (GABI_353G10), and *lecrk-I.8* (SALK_066416) were described previously (Gouhier-Darimont et al., 2019). Primers for genotyping insertion lines were designed with the SIGNAL T-DNA verification tool for all lines used in this study.

A dual sgRNA CRISPR Cas9 approach (Pauwels et al., 2018) was used to create a 33 kb deletion on chromosome 3 between *LecRK-I.1* (At3g45330) and *LecRK-I.6* (At3g45440), generating the sextuple mutant *ccI.1-I.6*. sgRNAs specific for *LecRK-I.1* and *LecRK-I.6* were selected using CRISPR-P (http://crispr.hzau.edu.cn/CRISPR2/). Complementary oligos with 4 bp overhangs were annealed and inserted in the Gateway ENTRY sgRNA shuttle vectors (Pauwels et al., 2018) pMR217 (L1-R5) for sgRNA-LecRK-I.1 and pMR218 (L5-L2) for

sgRNA-LecRK-I.6 via a cut-ligation reaction with BbsI (New England Biolabs) and T4 DNA ligase (New England Biolabs), generating two sgRNA modules pMR217-sgRNA-LecRK-I.1 and pMR218-sgRNA-LecRK-I.6. Using a Gateway Multisite LR reaction (Thermo Fisher), the two sgRNA modules were combined with pDE-Cas9Km (Pauwels et al., 2018) to get the final expression clone that was inserted in *Agrobacterium tumefaciens* strain GV3101 for transformation of Arabidopsis Col-0 by floral dipping. Seeds were selected on ½ MS with 50 µg/ml kanamycin under continuous day conditions for 12 days. Presence of a deletion was tested by PCR, using specific primers CC-LecRK-I.1-Rv and CC-LecRK-I.6-Fw flanking the deletion and generating a 465 bp fragment (Supplemental Fig. S11).

Oviposition and treatment with EE

For experiments with natural oviposition, plants were placed in a tent containing approximately 20 *P. brassicae* butterflies for a maximum of 8 h. Plants with 1 to 4 egg batches (min. 10 eggs/batch) were then kept in a growth chamber in plastic boxes for 4.5 days (just before hatching of the eggs). Control plants were exposed to the same conditions without butterflies.

P. brassicae eggs were collected and crushed with a pestle in Eppendorf tubes. After centrifugation (15,000 g, 3 min), the supernatant ('egg extract', EE) was collected and stored at -20°C. Plants were 4-5 weeks old at the time of treatment. For each plant, each of two leaves were treated with 2 µl of EE. This amount corresponds to one egg batch of ca. 20 eggs. A total of four plants were used for each experiment. After the appropriate time, EE was gently removed with a scalpel blade and treated leaves were stored in liquid nitrogen. Untreated plants were used as controls.

For GWAS, a large amount of EE was prepared as described and aliquots diluted 1:1 in deionized water were stored under N_2 at -80°C in order to ensure homogenous treatments during the entire experiment.

Genome-wide association study and haplotype analysis

For GWAS analysis, a set of 295 accessions from the RegMap panel (Horton et al., 2012) were used (Supplemental Table S1). Phenotyping was performed on weekly pools of 30 randomly selected accessions. Due to germination issues or poor growth of some accessions, phenotyping was carried over a total of 15 weeks. Because all accessions from a given pool could not be processed in a single day, accessions were phenotyped over two different days within a given week. In order to control for potential temporal effects during the experiment,

Col-0 plants originating from lab seed stock were sown every week and were phenotyped together with the other lines. For each accession, 3 leaves from 3 to 6 plants were treated with EE diluted 1:1 with deionized water leading to a total of 9 to 18 treated leaves. Treated plants were left in the growth chamber for an additional 5 days until phenotyping. After 5 days, treated leaves were removed with forceps, symptoms were scored, and pictures were taken as described below. Phenotypic data were averaged for each accession individually ("raw" symptom score) and used for mapping. In addition, normalized scores were calculated by dividing the score by the one of the Col-0 plants grown and phenotyped during the same week.

Mapping was performed locally on R (R-Core Development Team, 2005; Kerdaffrec et al., 2016) using an accelerated mixed model (AMM, Seren et al., 2012; Kerdaffrec et al., 2016) that accounts for population structure by computing a population-wide kinship matrix. Scripts and genotype/kinship matrices can be found on GitHub (https://github.com/Gregor-Mendel-Institute/dormancy/tree/master/kerdaffrec2016). Mapping was performed using the average symptom score or the normalized score for each accession. No cofactor was included in the model. Full imputed genotypes for 2029 lines (Togninalli et al., 2018) were used and only SNPs with a minor-allele frequency (MAF) > 0.05 were considered for analysis. After filtering, a total of 1,769,548 SNPs were used for mapping. To correct for genome-wide multiple testing, a Bonferroni corrected threshold of significance was computed by dividing $\alpha = 0.05$ by the number of SNPs used in the analysis. The percentage of variance explained by the top SNP (Chr. 3, 16633422) of *LecRK1-1* was calculated using the residual sum of squares (RSS) extracted from the GWA model. Weekly symptom scores of control Col-0 plants were rather stable (Supplemental Fig. S3A), with the exception of weeks 3, 7, and 8 where symptoms were lower or higher, respectively. When accession scores were normalized to their respective Col-0 control, GWA mapping revealed the same association on chromosome 2 as when using non-normalized score (Supplemental Fig. S3B and Fig. 2A), however the LecRK-I.1 locus on chromosome 3 is clearly visible when data from weeks 3, 7, and 8 are omitted (Supplemental Fig. S3C). Despite not reaching genome-wide significance, this locus features the highest association score besides the locus on chromosome 2. Since both loci are identified using normalized and non-normalized datasets, the rest of the analysis was carried-out using non-normalized symptom scores. This allows for a greater number of accessions to be included in the analysis (295 vs 226) and thus improves statistical power.

Haplotype analysis was based on the most significantly associated SNPs ($-\log_{10} P > 4$) using data extracted from the genotype matrix. Presence/absence of premature stop codons in

sequenced accessions (Supplemental Table S1) was recovered from the POLYMORPH1001 Variant browser (https://tools.1001genomes.org/polymorph/). Both sets of data were used to explore phenotypic data.

The population-wide cladogram was built by calculating the Euclidian distance between accessions from the kinship matrix, and clustering was subsequently performed using the "ward.d2" algorithm in R. Gene sequences in Fasta format from 125 accessions were obtained from SALK 1001 genome browser (http://signal.salk.edu/atg1001/3.0/gebrowser.php) and sequences were aligned using MAFFT for further analysis.

Sliding windows analyses of Tajima's D, Fu and Li's D / F on the LecRK-I.1 locus were performed using DnaSP (version 6.12.03) with sliding windows of 200 variant sites and a step size of 25 sites, and significance threshold was set according to a 95% confidence limit published before (Tajima, 1989; Fu and Li, 1993). Homologous gene sequences from *AtLecRK-I.1* in *Arabidopsis lyrata* were identified by BLAST, and the best hit was used as outgroup sequence for Fu and Li's statistics. 50 kb sliding-window analysis of Tajima's D was computed using VCF genotype file obtained from the 1001 Genome API (https://tools.1001genomes.org/api/index.html). Tajima's D was computed on sliding windows of 200 bp with a step size of 25 bp using custom-made R scripts.

Broad sense heritability and variance analysis

For each phenotype, broad sense heritability (H^2) was calculated using the following equations: $H^2 = V_g/V_p$ and $V_p = V_g + V_e$, where V_g, V_p, and V_e stand for genetic, phenotypic, and environmental variance, respectively. Since accessions are homozygous, V_e was estimated as the average intra-accession variance and V_p was the variance of the phenotype in the population.

Symptom scoring

Symptoms were scored visually from the adaxial side of the leaves and were classified into the following categories: no symptom (leaf treated area is still lush green, score = 0), small chlorosis (<50% of the treated area, score = 1), large chlorosis (> 50%, score = 2), small necrosis (brown spots or transparent membrane on < 50% of the treated area, score = 3), large necrosis (> 50%, score = 4), and spreading necrosis (necrosis not confined to the treated area, score = 5).

Histochemical staining

For quantification of cell death, EE or eggs were gently removed and leaves were submerged in lactophenol trypan blue solution (5 ml of lactic acid, 10 ml of 50% v/v glycerol, 1 mg of trypan blue [Sigma], and 5 ml of phenol) at 28°C for 2–3 h. After staining, leaves were destained for 10 min in boiling 95% (v/v) ethanol. Microscope images were saved as TIFF files and processed for densitometric quantification with ImageJ (version 1.48).

Salicylic acid quantification

SA quantification was performed using the bacterial biosensor *Acinetobacter sp*. ADPWH (Huang et al., 2005; Huang et al., 2006) according to (DeFraia et al., 2008; Zvereva et al., 2016). For each of 4 plants, EE or eggs were gently removed and six leaf discs (ca. 0.7 cm, ca. 20 mg) were collected, ground in liquid nitrogen, and extracted in 0.1M sodium acetate buffer (pH 5.6). Extracts were then centrifuged at 4°C for 15 min at 16,000 g. 50 µL of extract were incubated with 5 µL of β-Glucosidase from almonds (0.5 U/µl in acetate buffer, Sigma-Aldrich) during 90 min at 37°C to release SA from SA-glucoside (SAG). 20 µL of extract was then mixed with 60 µL of LB and 50 µL of a culture of *Acinetobacter* sp. ADPWH_lux (OD_{600} = 0.4), and incubated for 1 h at 37°C. Finally, luminescence was integrated using a 485 ± 10 nm filter for 1 s. A SA standard curve diluted in untreated *sid2-1* extract amounts ranging from 0 to 60 ng was read in parallel to allow quantification. SA amounts in samples were estimated by fitting a 3rd order polynomial regression on the standards.

Gene expression analysis

Analysis of gene expression by reverse transcription quantitative PCR was described previously (Bruessow et al., 2010; Gouhier-Darimont et al., 2013). Briefly, tissue samples were ground in liquid nitrogen, and total RNA was extracted using ReliaPrep™ RNA Tissue Miniprep (Promega) according to the manufacturer's instructions. Afterwards, cDNA was synthesized from 500 ng of total RNA using M-MLV reverse transcriptase (ThermoFisher) and subsequently diluted eightfold with water. Reactions were performed using Brilliant III Fast SYBR-Green QPCR Master Mix (Agilent) on a QuantStudio 3 real-time PCR instrument (ThermoFisher). Values were normalized to the housekeeping gene *SAND* (At2g28390). Primer efficiency was evaluated by five-step dilution regression. For each experiment, three biological replicates were analyzed. A list of all primers used in experiments can be found in Supplemental Table S2.

Publicly available RNA-seq data (GSE80744) from 728 accessions were recovered from the Gene Expression Omnibus repository (www.ncbi.nlm.nih.gov/geo/GEO). Expression data were then filtered to extract only values for accessions used in the study.

Homology modeling of kinase and ectodomain of LecRK-I.1

3D structure models were obtained by homology modeling through the Swiss model server (Waterhouse et al., 2018). The L-type lectin domain (extracellular part of the receptor) of LecRLK-I.1 was modeled using the crystal structure of *Spatholobus parviflorus* seed lectin (PDB ID: 3IPV, sequence identity 26%). The mannose molecule that is shown at the canonical carbohydrate-binding site is based on the structural superimposition with mannose and the structure of *Pisum arvense* lectin in complex with sugars (PDB ID: 5T7P). The kinase domain and the ATP at the catalytic cleft were obtained using as a template the crystal structure of BRASSINOSTEROID INSENSITIVE 1 kinase domain complexed with an ATP analog (PDB ID: 5LPV, sequence identity 37%). The molecular visualization software Pymol (The PyMOL Molecular Graphics System, Version 2.0 Schrödinger, LLC.) was used for structure analysis and graphic representation.

Statistical analyses

GWAS and subsequent analysis of the data obtained was performed with R software version 3.6. For boxplots, the thick line indicates the median, box edges represent 1st and 3rd quartile respectively, whiskers cover 1.5 times the interquartile space, and dots represent extreme values. Boxplot width is proportional to the number of samples. When displayed, notches indicate an approximate confidence interval for median values. All analyses using mutant lines, except SA quantifications, were analyzed using GraphPad Prism 8.0.1. ANOVAs were conducted by specifying treatment and/or genotype as factors. Multiple comparisons were performed using Dunnet's test when only comparisons to Col-0 were needed, and using Tukey's honestly significant difference (HSD) when all comparisons were required. SA data were analyzed with a linear mixed model using the lme4 package where replicate identity was included as a random factor. General linear hypothesis post-hoc test (GLHT) with Tukey or Dunnet contrasts was used for pairwise comparisons. Scoring data were analyzed using Kruskal-Wallis test followed by Dunn's test for multiple comparisons.

Accession numbers

Sequence data from this article can be found in TAIR (www.arabidopsis.org) under the following accession numbers:

LecRK-I.1 (At3g45330); *LecRK-I.2* (At3g45390); *LecRK-I.3* (At3g45410); *LecRK-I.4* (At3g45420); *LecRK-I.5* (At3g45430); *LecRK-I.6* (At3g45440); *LecRK-I.8* (At5g60280), *PR1* (At2g14610); *SAND* (At2g28390);

Supplemental Data

The following materials are available in the online version of this article.

Supplemental Figure S1. HR-like symptoms triggered by natural oviposition

Supplemental Figure S2. Setting-up conditions for the GWAS experiment

Supplemental Figure S3. GWA mapping using normalized symptom scores.

Supplemental Figure S4. Meta-analysis of association at the *LecRK-I.1* locus.

Supplemental Figure S5. Homology model of kinase and ectodomain of LecRK-I.1.

Supplemental Figure S6. Disruptive variation in *LecRK-I.1* does not correlate with symptoms.

Supplemental Figure S7. *LecRK-I.1* expression in 40 accessions with low or high symptom scores.

Supplemental Figure S8. Expression of genes in the vicinity of the *LecRK-I.1* locus.

Supplemental Figure S9. Map of *LecRK-I.1* haplotype distribution in European Arabidopsis accessions.

Supplemental Figure S10. Analysis of Tajima's D in a 50kb region around the *LecRK-I.1* locus.

Supplemental Figure S11. Deletion of the *LecRK-I.1*-*LecRK-I.6* cluster using CRISPR-Cas9.

Supplemental Table S1. List of the 295 Arabidopsis accessions used in this study.

Supplemental Table S2. List of primers used in this study.

ACKNOWLEDGMENTS

We would like to thank Esteban Alfonso for technical help and Blaise Tissot for maintenance of the plants. We thank Dany Buffat for his technical assistance during the screening. We are also grateful to Nicolas Salamin and Anna Marcionetti for advices regarding the selection analyses. We thank two anonymous reviewers for useful suggestions and comments. This work was supported by the Swiss National Science Foundation (grant no 31003A_169278 to

P.R. and 31003A_173101 to J.S.), EMBO (long term fellowship ALTF 248-2018 to E.K.), and Fondation de Famille Sandoz (to J.S and P.J.-S.).

FIGURE LEGENDS

Figure 1. Insect egg-induced HR-like response varies among natural Arabidopsis accessions. A, Representative picture of accessions (two leaves per accession) displaying varying phenotypes after treatment with *P. brassicae* egg extract (EE). B, Representative pictures of symptoms used for scoring in experiments. C, Proportion of each symptom class developed by some accessions shown in panel A as visualized from the adaxial side. 5 to 20 treated leaves of each ecotypes were used for scoring. D, Variation in HR-like response triggered after natural oviposition by *P. brassicae* butterflies. In all experiments shown here, duration of treatment was 5 days as this corresponds to the hatching time of naturally oviposited *P. brassicae* eggs. The dashed circles indicate the site of treatment on the abaxial side of the leaf. Leaves were digitally extracted for comparison.

Figure 2. Genome-wide mapping of insect-egg induced HR-like symptoms. A, Manhattan plot of the GWAS for symptom score after 5 days of *P. brassicae* EE treatment using a linear mixed model. Full imputed genotypes (1'769'548 SNPs) for all 295 accessions were used for mapping. Chromosomes are displayed in different colors and the dashed line indicates a significance level of 0.05 after Bonferroni correction for multiple testing. B, Local association plot of a 50 kb region surrounding the most significant marker. The x-axis represents the genomic position on chromosome 3 and color boxes indicate genes. Linkage desequilibrium (LD) to the most significant SNP (SNP3) is indicated by a color scale.

Figure 3. LecRK-I.1 plays a role in the induction of HR-like symptoms following EE treatment. A, Average symptom scores as visualized from the adaxial side after 5 days of treatment with EE. Means ± SE from three independent experiments are shown (n= 12-23 for each experiment). Stars indicate significant differences with Col-0 (Kruskal-Wallis followed by Dunn's test). B, Cell death as quantified by trypan blue staining after 3 days of EE treatment. Untreated leaves were used as controls (CTL). Means ± SE from 8-20 leaves are shown. This experiment was repeated once with similar results. Stars indicate significant differences with Col-0 (ANOVA followed by Dunnett's test). C, Total salicylic acid (SA + salicylic acid glucoside) after 3 days of EE treatment. Measurements were done using a bacterial biosensor, and untreated plants were used as controls. Means ± SE of two

independent experiments are shown (n= 4 for each experiment). Stars indicate significant differences with Col-0 (linerar mixed model (LMM) followed by Dunnet's test). *, $P<0.05$; **, $P<0.01$.

Figure 4. LecRK-I.1 plays a role in the induction of HR-like symptoms following *P. brassicae* oviposition. A, Average symptom scores as visualized from the adaxial side. Means ± SE from three independent experiments are shown (n= 7-20 for each experiment). B, Cell death as quantified by trypan blue (TB) staining. Means ± SE from three independent experiments are shown (n= 5 for each experiment). C, Total salicylic acid (SA + SAG) measurement using a bacterial biosensor. Means ± SE of three independent experiments are shown (n= 4 for each experiment). Analyses were done 4.5 days after oviposition (OVI). Untreated plants were used as controls (CTL). Letters indicate significant differences at $P<0.05$ (LMM followed by Tukey's honestly significant difference (HSD) test).

Figure 5. Local association and haplotype analysis of the *LecRK-I.1* locus. A, Local association plot of the *LecRK-I.1* locus. The x-axis represents the genomic position on chromosome 3. LD of markers ($-\log_{10} P>4$) to the most significant SNP (SNP3) is indicated by a color scale. The dashed line indicates the Bonferroni corrected significance threshold at $\alpha=0.05$. B, Gene and protein domain organization according to UNIPROT. C, Haplotype analysis using the five most significant SNPs in the *LecRK-I.1* gene. Mean symptom score ± SE is shown and n indicates the number of accessions carrying each haplotype. Different letters indicate significant difference at $P<0.05$ (ANOVA, followed by Tukey's HSD for multiple comparison). The coordinates on chromosome 3 of SNP1-5 displayed in panel A are the following: SNP1: 16632685; SNP2: 16632698; SNP3: 16633422; SNP4: 16633802; SNP5: 16633802.

Figure 6. Natural *LecRK-I.1* haplotypes are expressed similarly upon EE treatment and expression does not correlate with symptom score. A, *LecRK-I.1* expression in 40 different accessions with low and high symptoms after 72 h of EE treatment. Transcript levels were plotted according to haplotypes defined in Fig. 4. Different letters indicate significant difference at $P<0.05$ (ANOVA, followed by Tukey's HSD for multiple comparison). Thick line indicates the median, box edges represent 1st and 3rd quartile respectively, whiskers cover 1.5 times the interquartile space, and dots represent extreme values. B, *LecRK-I.1* expression in accessions with low or high symptoms does not correlate with symptom scores

of the respective accessions. Gene expression was monitored by RT-qPCR and target gene transcript level was normalized to the reference gene *SAND*. Means of three technical replicates are shown. Expression data were corrected by adding half the smallest non-zero value in order to avoid zero values, and $\log_{10}$-transformed prior to analysis. ns, not significant (ANOVA, $P>0.05$). Pearson correlation coefficient (r) and corresponding P value (*P*) between *LecRK-I.1* transcript level and symptom score are shown.

Figure 7. Signatures of selection at the *LecRK-I.1* locus. A, Frequency of the different haplotypes in the accession panel used for GWAS mapping. B, Cladogram constructed from a genome-wide kinship matrix of the 295 accessions used for GWAS. The outermost circle indicates the haplotype carried by a given accession. C, Sliding window analysis of Tajima's D, and Fu and Li's D and F statistics along the *LecRK-I.1* coding region using a window size of 200 variant sites and a step size of 25 sites. A subset of 125 accessions with available full genome sequences was used for this analysis. The red dashed line indicates significance threshold at $P<0.05$. The gene structure of *LecRK-I.1* is shown below.

Figure 8. *LecRK-I.1* genetically interacts with *LecRK-I.8*. A, Col-0, single and double *lecrk* mutants were treated with EE. Average symptom score was visualized from the adaxial side after 5 days of EE treatment. Mean ± SE from three independent experiment is shown (n=12-23 for each experiment). Different letters indicate significant difference at $P< 0.05$ (Kruskal-Wallis followed by Dunn's test). B, Cell death as quantified by trypan blue staining after 3 days of EE treatment. Untreated leaves were used as controls. Means ± SE from 8-20 leaves are shown. This experiment was repeated once with similar results. Different letters indicate significant difference at $P< 0.05$ (ANOVA followed by Tukey's HSD test). C, Expression of the marker gene *PR1* after 3 days of EE treatment. Transcript levels were monitored by RT-qPCR and normalized to the reference gene *SAND*. Means ± SE of three technical replicates are shown. This experiment was repeated twice with similar results. Different letters indicate significant difference at $P< 0.05$ (ANOVA followed by Tukey's HSD test). D, Total salicylic acid (SA + SAG) after 3 days of EE treatment. Measurements were done using a bacterial biosensor, untreated plants were used as control. Means ± SE of three independent experiments are shown (n=4 for each experiment). Different letters indicate significant difference at $P< 0.05$ (LMM followed by Tukey's HSD test).

Parsed Citations

Ariga H, Katori T, Tsuchimatsu T, Hirase T, Tajima Y, Parker JE, Alcázar R, Koornneef M, Hoekenga O, Lipka AE, et al (2017) NLR locus-mediated trade-off between abiotic and biotic stress adaptation in Arabidopsis. Nature Plants 3: 17072
Google Scholar: Author Only Title Only Author and Title

Bakker EG, Toomajian C, Kreitman, M, Bergelson J (2006) A genome-wide survey of R gene polymorphisms in Arabidopsis. Plant Cell 18: 1803–1818
Google Scholar: Author Only Title Only Author and Title

Bellande K, Bono JJ, Savelli B, Jame E, Canut H (2017) Plant lectins and lectin receptor-like kinases: How do they sense the outside? International Journal of Molecular Sciences 18: 1164

Bittner N, Trauer-Kizilelma U, Hilker M (2017) Early plant defence against insect attack: involvement of reactive oxygen species in plant responses to insect egg deposition. Planta 245: 993–1007
Google Scholar: Author Only Title Only Author and Title

Blenn B, Bandoly M, Küffner A, Otte T, Geiselhardt S, Fatouros NE, Hilker, M (2012) Insect egg deposition induces indirect defense and epicuticular wax changes in Arabidopsis thaliana. Journal of Chemical Ecology 38: 882–92
Google Scholar: Author Only Title Only Author and Title

Bonnet C, Lassueur S, Ponzio C, Gols R, Dicke M, Reymond P (2017) Combined biotic stresses trigger similar transcriptomic responses but contrasting resistance against a chewing herbivore in Brassica nigra. BMC Plant Biology 17: 127
Google Scholar: Author Only Title Only Author and Title

Bouwmeester K, Govers F (2009) Arabidopsis L-type lectin receptor kinases: Phylogeny, classification, and expression profiles. Journal of Experimental Botany 60: 4383–4396
Google Scholar: Author Only Title Only Author and Title

Bruessow F, Gouhier-Darimont C, Bruchala A, Metraux J-P, Reymond, P (2010) Insect eggs suppress plant defence against chewing herbivores. Plant Journal 62: 876–885
Google Scholar: Author Only Title Only Author and Title

Chen YH, Gols R, Benrey B (2015) Crop domestication and its impact on naturally selected trophic interactions. Annual Review of Entomology 60: 35–58
Google Scholar: Author Only Title Only Author and Title

Choi J, Tanaka K, Cao Y, Qi Y, Qiu J, Lian Y, Lee SY, Stacey G (2014) Identification of a plant receptor for extracellular ATP. Science 343: 290–294
Google Scholar: Author Only Title Only Author and Title

DeFraia CT, Schmelz EA, Mou Z (2008) A rapid biosensor-based method for quantification of free and glucose-conjugated salicylic acid. Plant Methods 4: 28
Google Scholar: Author Only Title Only Author and Title

Delph LF, Kelly JK (2014) On the importance of balancing selection in plants. New Phytologist 201: 45–56
Google Scholar: Author Only Title Only Author and Title

Desurmont GA, Weston PA (2011) Aggregative oviposition of a phytophagous beetle overcomes egg-crushing plant defences. Ecological Entomology 36: 335–343
Google Scholar: Author Only Title Only Author and Title

Doss RP, Oliver JE, Proebsting WM, Potter SW, Kuy S, Clement SL, Williamson RT, Carney JR, DeVilbiss ED (2000) Bruchins: Insect-derived plant regulators that stimulate neoplasm formation. Proceedings of the National Academy of Sciences USA 97: 6218–6223
Google Scholar: Author Only Title Only Author and Title

Fatouros NE, Cusumano A, Danchin EGJ, Colazza S (2016) Prospects of herbivore egg-killing plant defenses for sustainable crop protection. Ecology and Evolution 6: 6906–6918
Google Scholar: Author Only Title Only Author and Title

Fatouros NE, Lucas-Barbosa D, Weldegergis BT, Pashalidou FG, van Loon JJA, Dicke M, Harvey JA, Gols R, Huigens ME (2012) Plant volatiles induced by herbivore egg deposition affect insects of different trophic levels. PLoS One 7: e43607
Google Scholar: Author Only Title Only Author and Title

Fatouros NE, Pineda,A, Huigens ME, Broekgaarden C, Shimwela MM, Candia IAF, Verbaarschot P, Bukovinszky T (2014) Synergistic effects of direct and indirect defences on herbivore egg survival in a wild crucifer. Proceedings of the Royal Society B Biological Sciences 281: 20141254
Google Scholar: Author Only Title Only Author and Title

Fu YX, Li WH (1993) Statistical tests of neutrality of mutations. Genetics 133: 693–709
Google Scholar: Author Only Title Only Author and Title

Garza R, Vera J, Cardona C, Barcenas N, Singh SP (2001) Hypersensitive response of beans to Apion godmani (Coleoptera:

Curculionidae). Journal of Economic Entomology 94: 958–962
Google Scholar: Author Only Title Only Author and Title

Geuss D, Stelzer S, Lortzing T, Steppuhn A (2017) Solanum dulcamara's response to eggs of an insect herbivore comprises ovicidal hydrogen peroxide production. Plant, Cell and Environment 40: 2663–2677
Google Scholar: Author Only Title Only Author and Title

Gilardoni PA, Hettenhausen C, Baldwin IT, Bonaventure G (2011) Nicotiana attenuata lectin receptor kinase1 suppresses the insect-mediated inhibition of induced defense responses during Manduca sexta herbivory. Plant Cell 23: 3512–353
Google Scholar: Author Only Title Only Author and Title

Gouget A, Senchou V, Govers F, Sanson A, Barre A, Rougé P, Pont-Lezica R, Canut H (2006) Lectin receptor kinases participate in protein-protein interactions to mediate plasma membrane-cell wall adhesions in Arabidopsis. Plant Physiology 140: 81–90.
Google Scholar: Author Only Title Only Author and Title

Gouhier-Darimont C, Schmiesing, A, Bonnet C, Lassueur S, Reymond P (2013) Signalling of Arabidopsis thaliana response to Pieris brassicae eggs shares similarities with PAMP-triggered immunity. Journal of Experimental Botany 64: 665–74
Google Scholar: Author Only Title Only Author and Title

Gouhier-Darimont C, Stahl E, Glauser G, Reymond P (2019) The Arabidopsis lectin receptor kinase LecRK-I.8 is involved in insect egg perception. Frontiers in Plant Science 10: 623
Google Scholar: Author Only Title Only Author and Title

Griese E, Pineda A, Pashalidou FG, Pizarro Iradi E, Hilker M, Dicke M, Fatouros NE (2020) Plant responses to butterfly oviposition partly explain preference–performance relationships on different brassicaceous species. Oecologia 192: 463-475
Google Scholar: Author Only Title Only Author and Title

Hilker M, Fatouros NE (2015) Plant responses to insect egg deposition. Annual Review of Entomology 60: 493–515
Google Scholar: Author Only Title Only Author and Title

Hilker M, Meiners T (2006) Early herbivore alert: insect eggs induce plant defense. Journal of Chemical Ecology 32: 1379–97
Google Scholar: Author Only Title Only Author and Title

Hofberger JA, Nsibo DL, Govers F, Bouwmeester K, Schranz ME (2015) A complex interplay of tandem- and whole-genome duplication drives expansion of the L-type lectin receptor kinase gene family in the Brassicaceae. Genome Biology and Evolution 7: 720–734
Google Scholar: Author Only Title Only Author and Title

Horton MW, Hancock AM, Huang YS, Toomajian C, Atwell S, Auton A, Muliyati NW, Platt A, Sperone FG, Vilhjálmsson BJ, et al (2012) Genome-wide patterns of genetic variation in worldwide Arabidopsis thaliana accessions from the RegMap panel. Nature Genetics 44: 212–216
Google Scholar: Author Only Title Only Author and Title

Huang WE, Huang L, Preston M, Naylor, M, Carr JP, Li Y, Singer AC, Whiteley AS, Wang H (2006) Quantitative in situ assay of salicylic acid in tobacco leaves using a genetically modified biosensor strain of Acinetobacter sp. ADP1. Plant Journal 46: 1073–1083
Google Scholar: Author Only Title Only Author and Title

Huang WE, Wang H, Zheng H, Huang L, Singer AC, Thompson I, Whiteley AS (2005) Chromosomally located gene fusions constructed in Acinetobacter sp. ADP1 for the detection of salicylate. Environmental Microbiology 7: 1339–1348
Google Scholar: Author Only Title Only Author and Title

Huang PY, Yeh YH, Liu AC, Cheng CP, Zimmerli L (2014) The Arabidopsis LecRK-VI.2 associates with the pattern-recognition receptor FLS2 and primes Nicotiana benthamiana pattern-triggered immunity. Plant Journal 79: 243–255
Google Scholar: Author Only Title Only Author and Title

Huard-Chauveau C, Perchepied L, Debieu M, Rivas S, Kroj T, Kars I, Bergelson J, Roux F, Roby D (2013) An atypical kinase under balancing selection confers broad-spectrum disease resistance in Arabidopsis. PLoS Genetics 9: e1003766
Google Scholar: Author Only Title Only Author and Title

Kalske A, Muola A, Mutikainen P, Leimu R (2014) Preference for outbred host plants and positive effects of inbreeding on egg survival in a specialist herbivore. Proceedings of the Royal Society B Biological Sciences 281: 20141421
Google Scholar: Author Only Title Only Author and Title

Kerdaffrec E, Filiault DL, Korte A, Sasaki E, Nizhynska V, Seren Ü, Nordborg M (2016) Multiple alleles at a single locus control seed dormancy in Swedish Arabidopsis. eLife 5: 1–24
Google Scholar: Author Only Title Only Author and Title

Kutschera A, Dawid C, Gisch N, Schmid C, Raasch L, Gerster T, Schäffer M, Smakowska-Luzan E, Belkhadir Y, Vlot AC, et al (2019) Bacterial medium-chain 3-hydroxy fatty acid metabolites trigger immunity in Arabidopsis plants. Science 181: 178–181
Google Scholar: Author Only Title Only Author and Title

Li L, Kim P, Yu L, Cai G, Chen S, Alfano JR, Zhou, JM (2016). Activation-dependent destruction of a co-receptor by a Pseudomonas syringae effector dampens plant immunity. Cell Host & Microbe 20: 504-514
Google Scholar: Author Only Title Only Author and Title

Little D, Gouhier-Darimont C, Bruessow F, Reymond P (2007) Oviposition by pierid butterflies triggers defense responses in Arabidopsis. Plant Physiology 143: 784–800
Google Scholar: Author Only Title Only Author and Title

Liu Y, Wu H, Chen H, Liu Y, He J, Kang H, Sun Z, Pan G, Wang Q, Hu J, et al (2015) A gene cluster encoding lectin receptor kinases confers broad-spectrum and durable insect resistance in rice. Nature Biotechnology 33: 301–305
Google Scholar: Author Only Title Only Author and Title

Miya A, Albert P, Shinya T, Desaki Y, Ichimura K, Shirasu K, Narusaka Y, Kawakami N, Kaku H, Shibuya N (2007) CERK1, a LysM receptor kinase, is essential for chitin elicitor signaling in Arabidopsis. Proceedings of the National Academy of Sciences USA 104: 19613–19618
Google Scholar: Author Only Title Only Author and Title

Morales J, Kadota Y, Zipfel C, Molina A, Torres M (2016) The Arabidopsis NADPH oxidases RbohD and RbohF display differential expression patterns and contributions during plant immunity. Journal of Experimental Botany 67: 1663-76
Google Scholar: Author Only Title Only Author and Title

Paniagua Voirol LR, Valsamakis G, Lortzing V, Weinhold A, Johnston PR, Fatouros NE, Kunze R, Hilker M (2020) Plant responses to insect eggs are not induced by egg-associated microbes, but by a secretion attached to the eggs. Plant Cell & Environment 43: 1815–1826
Google Scholar: Author Only Title Only Author and Title

Pauwels L, De Clerck R, Goossens J, Iñigo S, Williams C, Ron M, Britt A, Goossens A (2018) A dual sgRNA approach for functional genomics in Arabidopsis thaliana. Genes Genomes Genetics 8: 2603-2615
Google Scholar: Author Only Title Only Author and Title

Petzold-Maxwell J, Wong S, Arellano C, Gould F (2011) Host plant direct defence against eggs of its specialist herbivore, Heliothis subflexa. Ecology and Entomology 36: 700–70
Google Scholar: Author Only Title Only Author and Title

Pham AQ, Cho SW, Nguyen CT, Stacey G (2020) Arabidopsis Lectin Receptor Kinase P2K2 is a second plant receptor for extracellular ATP and contributes to innate immunity. Plant Physiology 183: 1363-1375
Google Scholar: Author Only Title Only Author and Title

R Development Core Team (2005) R: A language and environment for statistical computing. R Foundation for Statistical Computing, Vienna, Austria. ISBN 3-900051-07-0, URL: http://www.R-project.org
Google Scholar: Author Only Title Only Author and Title

Reymond P (2013) Perception, signaling and molecular basis of oviposition-mediated plant responses. Planta 238: 247–58
Google Scholar: Author Only Title Only Author and Title

Reymond P, Weber H, Damond M, Farmer EE (2000) Differential gene expression in response to mechanical wounding and insect feeding in Arabidopsis. Plant Cell 12: 707-720
Google Scholar: Author Only Title Only Author and Title

Seino Y, Suzuki Y, Kazushige S (1996) An Ovicidal Substance Produced by Rice Plants in Response to Oviposition by the Whitebacked Planthopper, Sogatella furcifera (HORVÀTH) (Homoptera: Delphacidae). Applied Entomology and Zoology 31: 467-473
Google Scholar: Author Only Title Only Author and Title

Seren Ü,Vilhjálmsson BJ, Horton MW, Meng D, Forai P, Huang YS, Long Q, Segura V, Nordborg M (2012) GWAPP: A Web Application for Genome-Wide Association Mapping in Arabidopsis. Plant Cell 24: 4793–4805
Google Scholar: Author Only Title Only Author and Title

Shapiro AM, DeVay JE (1987) Hypersensitivity reaction of Brassica nigra L. (Cruciferae) kills eggs of Pieris butterflies (Lepidoptera: Pieridae). Oecologia 71: 631–632
Google Scholar: Author Only Title Only Author and Title

Stahl E, Brillatz T, Ferreira Queiroz E, Marcourt L, Schmiesing A, Hilfiker O, Riezman I, Riezman H, Wolfender J-L, Reymond P (2020) Phosphatidylcholines from Pieris brassicae eggs induce an immune response in Arabidopsis. eLife 9: e60293
Google Scholar: Author Only Title Only Author and Title

Tajima F (1989) Statistical method for testing the neutral mutation hypothesis by DNA polymorphism. Genetics 123: 585–595
Google Scholar: Author Only Title Only Author and Title

Takahashi F, Yoshida R, Ichimur K, Mizoguchi, T, Seo S, Yonezawa,M, Maruyama K, Yamaguchi-Shinozaki K, Shinozaki K (2007) The mitogen-activated protein kinase cascade MKK3–MPK6 is an important part of the jasmonate signal transduction pathway in Arabidopsis. Plant Cell 19: 805–818
Google Scholar: Author Only Title Only Author and Title

Tamiru A, Khan ZR, Bruce TJA (2015) New directions for improving crop resistance to insects by breeding for egg induced defence. Current Opinion in Insect Science 9: 51-55
Google Scholar: Author Only Title Only Author and Title

Tamiru A, Paliwal R, Manthi SJ, Odeny DA, Midega CAO, Khan ZR, Pickett JA, Bruce TJA (2020) Genome wide association analysis of a

stemborer egg induced "call-for-help" defence trait in maize. Scientific Reports 10: 11205
Google Scholar: Author Only Title Only Author and Title

Taylor SS, Kornev AP (2011). Protein kinases: evolution of dynamic regulatory proteins. Trends in Biochemical Sciences 36: 65-77
Google Scholar: Author Only Title Only Author and Title

Togninalli M, Seren Ü, Meng D, Fitz J, Nordborg M, Weigel D, Borgwardt K, Korte A, Grimm DG (2018) The AraGWAS Catalog: a curated and standardized Arabidopsis thaliana GWAS catalog. Nucleic Acids Research 46: D1150–D1156
Google Scholar: Author Only Title Only Author and Title

Torres MA, Dangl JL, Jones JDG (2002) Arabidopsis gp91phox homologues AtrbohD and AtrbohF are required for accumulation of reactive oxygen intermediates in the plant defense response. Proceedings of the National Academy of Sciences USA 99: 517–522
Google Scholar: Author Only Title Only Author and Title

van Velzen E, Etienne RS (2015) The importance of ecological costs for the evolution of plant defense against herbivory. Journal of Theoretical Biology 372: 89–9
Google Scholar: Author Only Title Only Author and Title

Vila-Aiub MM, Neve P, Roux F (2011) A unified approach to the estimation and interpretation of resistance costs in plants. Heredity 107: 386–394.
Google Scholar: Author Only Title Only Author and Title

Wang C, Huang X, Li Q, Zhang Y, Li JL, Mou Z (2019) Extracellular pyridine nucleotides trigger plant systemic immunity through a lectin receptor kinase/BAK1 complex. Nature Communications 10: 4810
Google Scholar: Author Only Title Only Author and Title

Wang C, Zhou M, Zhang X, Yao J, Zhang Y, Mou Z (2017) A lectin receptor kinase as a potential sensor for extracellular nicotinamide adenine dinucleotide in Arabidopsis thaliana. eLife 6: e2547
Google Scholar: Author Only Title Only Author and Title

Wang Y, Bouwmeester K (2017) L-type lectin receptor kinases: New forces in plant immunity. PLoS Pathogens 13: e1006433
Google Scholar: Author Only Title Only Author and Title

Waterhouse A, Bertoni M, Bienert S, Studer G, Tauriello G, Gumienny R, Heer FT, de Beer TAP, Rempfer C, Bordoli L, et al (2018). SWISS-MODEL: homology modeling of protein structures and complexes. Nucleic Acids Research 46: W296-W303
Google Scholar: Author Only Title Only Author and Title

Wu Q, Han TS, Chen X, Chen JF, Zou YP, Li ZW, Xu YC, Guo YL (2017) Long-term balancing selection contributes to adaptation in Arabidopsis and its relatives. Genome Biology 18: 1–15
Google Scholar: Author Only Title Only Author and Title

Yamasaki M, Yoshimura A, Yasui H (2003) Genetic basis of ovicidal response to whitebacked planthopper (Sogatella furcifera Horváth) in rice (Oryza sativa L.). Molecular Breeding 12: 133–143
Google Scholar: Author Only Title Only Author and Title

Yang Y, Xu J, Leng Y, Xiong G, Hu J, Zhang G, Huang L, Wang L, Guo L, Li J, et al (2014) Quantitative trait loci identification, fine mapping and gene expression profiling for ovicidal response to whitebacked planthopper (Sogatella furcifera Horvath) in rice (Oryza sativa L.). BMC Plant Biol 14: 145
Google Scholar: Author Only Title Only Author and Title

Yang R (2017) Genome-wide estimation of heritability and its functional components for flowering, defense, ionomics, and developmental traits in a geographically diverse population of Arabidopsis thaliana. Genome 60: 572–580
Google Scholar: Author Only Title Only Author and Title

Zhou J, Wang P, Claus LA, Savatin DV, Xu G, Wu S, Meng X, Russinova E, He P, Shan L (2019). Proteolytic processing of SERK3/BAK1 regulates plant immunity, development, and cell death. Plant Physiology 180: 543-558
Google Scholar: Author Only Title Only Author and Title

Zvereva AS, Golyaev V, Turco S, Gubaeva EG, Rajeswaran R, Schepetilnikov MV, Srour O, Ryabova LA, Boller T, Pooggin MM (2016) Viral protein suppresses oxidative burst and salicylic acid-dependent autophagy and facilitates bacterial growth on virus-infected plants. New Phytologist 211: 1020–1034
Google Scholar: Author Only Title Only Author and Title